

Compact and sustainable electronic module for silicon photodetectors

A. Sadigov^{1,2}, S. Nuruyev^{2,3}, R. Akbarov^{1,2,3},
D.B. Berikov^{3,4}, A. Madadzada^{1,3}, A. Mammadli²,
S. Lyubchyk⁵, E. Yilmaz⁶

¹Innovation and Digital Development Agency Nuclear Research Department, Baku, Azerbaijan

²Institute of Radiation Problems under Ministry of Science and Education, Baku, Azerbaijan

³Joint Institute for Nuclear Research, Dubna, Russia

⁴Institute of Nuclear Physics of the Ministry of Energy of the Republic of Kazakhstan, Almaty, Kazakhstan

⁵Universidade Lusofona, 1749-024 Lisboa, Portugal

⁶Department of Physics, Bolu Abant Izzet Baysal University, Bolu, Turkiye

E-mail: sebuhinuruyev@jinr.ru

DOI: 10.32523/ejpfm.2023070302

Received: 20.09.2023 - after revision

This article presents the development of a cost-effective and efficient electronic module for silicon photodetectors (SiPM). The electronic module combines essential functionalities, such as a high voltage power supply, a preamplifier, and a signal comparator, into a compact circuit. A high voltage power supply with a range of 30 to 140 V provides a stable bias voltage with 0.01 V accuracy, while a preamplifier with 40 gain and 250 MHz bandwidth enables signal amplification necessary to extract weak signals. The comparator converts an analogue signal (higher than 8 mV) into TTL (transistor-transistor logic), which makes it easy to process and analyze with digital devices such as microcontrollers or make it possible to send signals over long distances by a cable. The module has been tested using an LYSO scintillator and a silicon photomultiplier (SiPM) called a micropixel avalanche photodiode (MAPD). It provides a more effective and efficient solution for reading out signals from SiPMs in a variety of applications, delivering reliable and accurate results in real-time.

Keywords: silicon photodetectors; SiPM; micropixel avalanche photodiodes; DC-DC converter; signal comparator; preamplifier

Introduction

Nowadays, silicon photomultipliers (SiPMs) have emerged as solid-state photodetectors with immense potential, serving as compelling alternatives to vacuum photomultipliers (PMTs) across a broad spectrum of applications [1-4]. SiPMs come with a multitude of advantages, notably their robustness, fast response times, low operating voltage requirements, and compactness [5-8]. These attributes have propelled the widespread adoption of SiPMs in diverse fields, encompassing particle physics, astrophysics, nuclear physics, medicine, and public security applications [9-15].

Within high-energy particle experiments, SiPMs are indispensable devices for the detection of various types of particles [16]. They also find utility in specialized detectors designed for the observation of faint astronomical phenomena, such as gamma-ray bursts and supernovae [17]. In the field of nuclear physics, SiPMs contribute to the precise measurement of reactor antineutrino spectra [18] and are widely used in small-angle and wide-angle X-ray scattering (SAXS and WAXS), as well as small-angle neutron scattering (SANS) [19, 20]. Furthermore, SiPMs play a pivotal role in medical diagnostics, particularly in Positron Emission Tomography (PET) imaging, obtaining detailed body images with remarkable precision [21].

While these applications frequently employ Specific Integrated Circuits (ASICs) to handle the substantial number of output channels generated by SiPM arrays, they prove impractical for experiments with low channel density requirements. To address this challenge, a compact and sustainable electronic module has been developed specifically for SiPM readout systems. This module integrates functionalities, including bias supply, discriminator, and amplifier, into a single circuit. Consequently, it simplifies the overall circuitry and enhances the usability of SiPMs in various experiments.

Aim of this article is development of a compact and sustainable electronic module for silicon photomultipliers.

Electronic module

The module is a versatile device designed to cater to various applications where different SiPMs are used. The aim of this section is to shed light on possibilities of the module through a comprehensive analysis of its parts.

This module encompasses a DC-DC voltage converter, a preamplifier, and a comparator that converts analogue signal to TTL. Each component of the module plays a crucial role in enhancing functionality and performance. In this article, we delve into the intricate details of each component, examining their functionalities, design principles, and performance characteristics.

The high voltage converter

The DC-DC step-up high-voltage converter exhibits exceptional stability, maintaining a low average output voltage fluctuation of less than 10 mV. The circuit

diagram of DC-DC circuit was shown in in Figure 1.

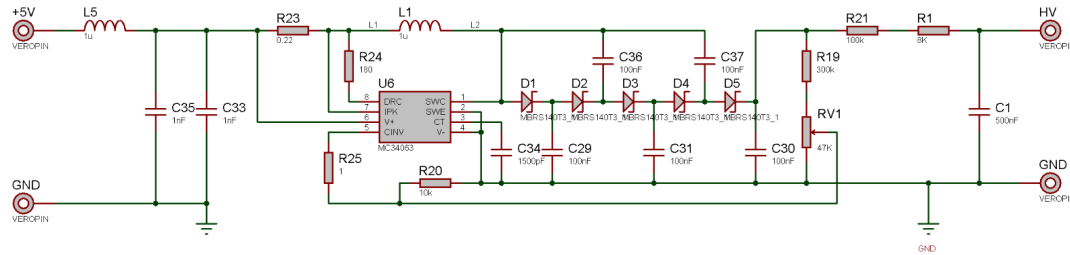


Figure 1. The high voltage converter circuit diagram.

MC34063A was used as duty cycle oscillator with a steady 10500 Hz frequency. The energy collected within the inductance was then discharged into capacitors through cascades, each consisting of pairs of diodes and capacitors. As these charged capacitors discharged, the output voltage surged in proportion to the voltage stored in the capacitors. By this way, it is possible to increase the output voltage by increasing the number of capacitors and diode pairs at a given frequency. An additional voltage divider is assembled to change (decrease and increase) the applied voltage in a voltage interval of 10 V. The maintenance of output voltage stability was achieved through the incorporation of Zenner diodes. Furthermore, we harnessed the feedback channel of the MC34063A to secure the independence of the output voltage from fluctuations in the input voltage. This ensured a constant output value even when the input signal varies within the range of 3-10 V.

The IC circuit was initially simulated using ISIS 7 Professional Proteus software and later assembled on the board. Special attention was given to minimizing current loss during the selection of components. The current consumption of the DC-DC was 2 mA [22].

The preamplifier

The preamplifier for SiPMs with NPN and PNP transistors is designed to convert the weak photocurrent signals from SiPMs and SiPM based detectors into amplified voltage signals. It provides a gain of 40 and a bandwidth of 250 MHz, allowing for accurate and efficient signal amplification suitable for silicon photo-multiplier applications. This is important for all types of scintillators with decay time more than 40 ns. Additionally, the preamplifier can increase its bandwidth up to 500 MHz with minimal adjustments. Figure 2 shows the circuit diagram and the final form of the assembled preamplifier.

The comparator

Signal comparator was implemented to convert the negative analogue output signal from the preamplifier to TTL levels. An analog-to-TTL converter was assembled using an AD8007 operational amplifier. Figure 3 shows the circuit diagram and the final form of the comparator.

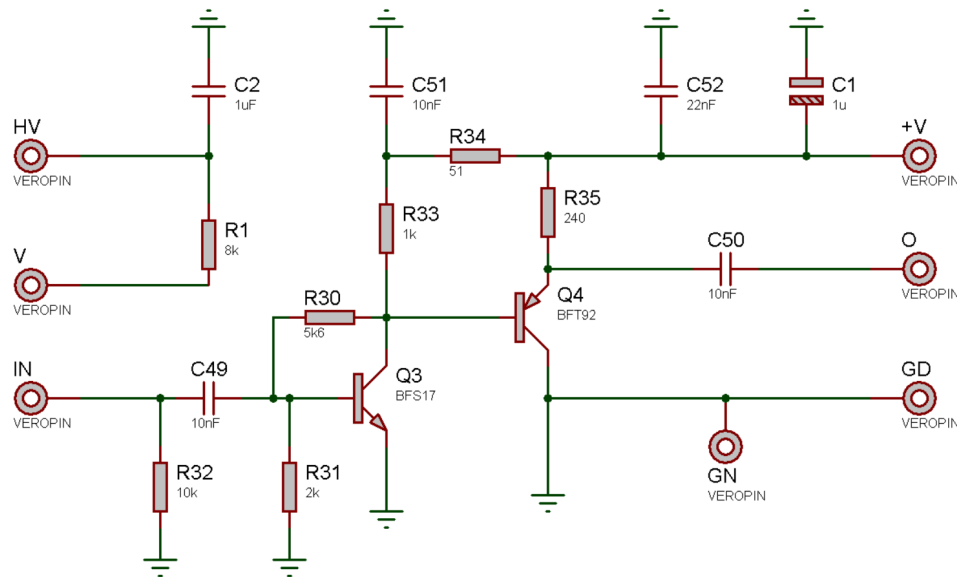


Figure 2. The circuit diagram of the preamplifier.

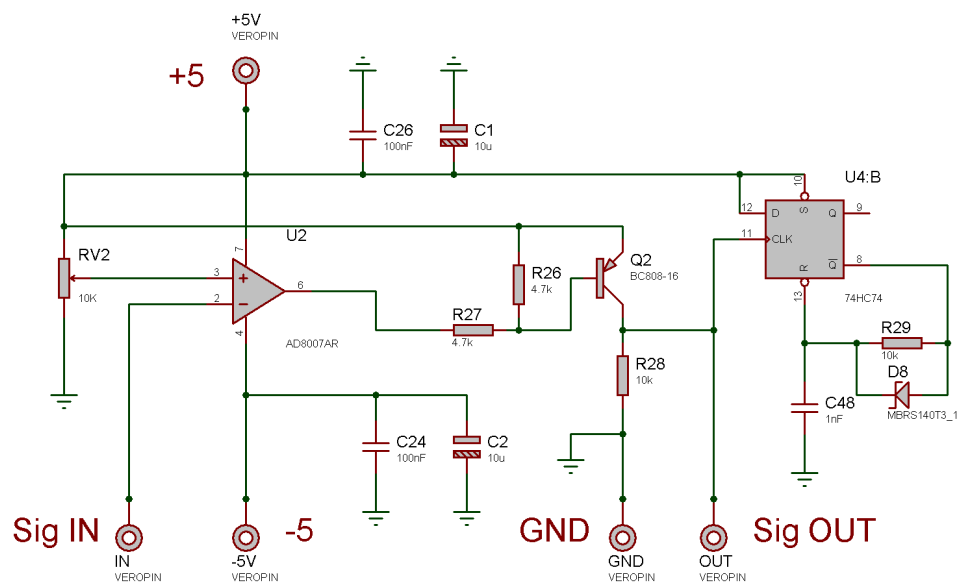


Figure 3. The circuit diagram of the comparator.

The analogue signal received from the preamplifier was connected to the input of the comparator. The threshold level for the input signal was determined using a pot resistor. If the input signal exceeded the threshold value (set at 8 mV), input signal was compared to the reference one, resulting in a square signal at the output. When the input signal amplitude was below the threshold, no signal was observed at the output, which was held at a logic low state (0). A transistor was used to maintain a constant output signal of the comparator. This arrangement ensured that the output signals had a consistent amplitude level. This 74HC74 flip-flop helped maintain a constant width for the output signal. Time shift between two inputs of the flip-flop defines the widths of the output signal.

Electronic module testing

The functionality of the module was tested using the scintillation detector based on the MAPD and LYSO scintillator. To minimize light loss, the scintillator was enveloped with multiple layers of white Teflon tape on all sides, leaving only the side connected to the MAPD [23]. For better optical contact between the scintillator and MAPD, a special optical lubricant was used. The ^{137}Cs calibration source was placed on the surface of the LYSO scintillator. A CAEN DT5720 multichannel desktop signal digitizer with a sampling rate of 250 MHz was used as an analysis and recording device. The measurements were carried out in a so-called dark box, to isolate the detector from ambient light, at room temperature (Figure 4).

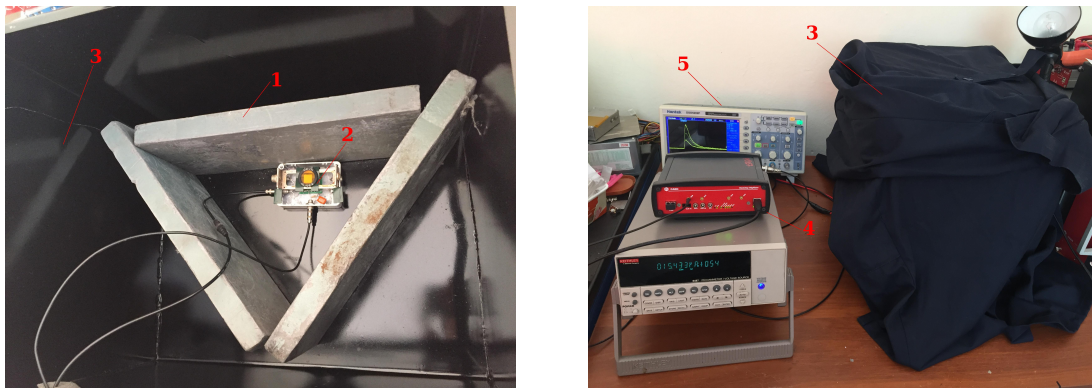


Figure 4. Setup for testing the electronic module. 1 – lead shield to reduce the background, 2 – detector connected to the module, 3 – dark box, 4 – desktop digitizer CAEN, 5 – oscilloscope.

The output signal of the module branched: one output was fed to an oscilloscope for visual observation of pulses (Figure 5), the other to a digitizer. Then the digitized signal was sent to a personal computer for data accumulation and their subsequent analysis. Subsequent analysis of the waveform data was carried out using scripts written in the ROOT environment.

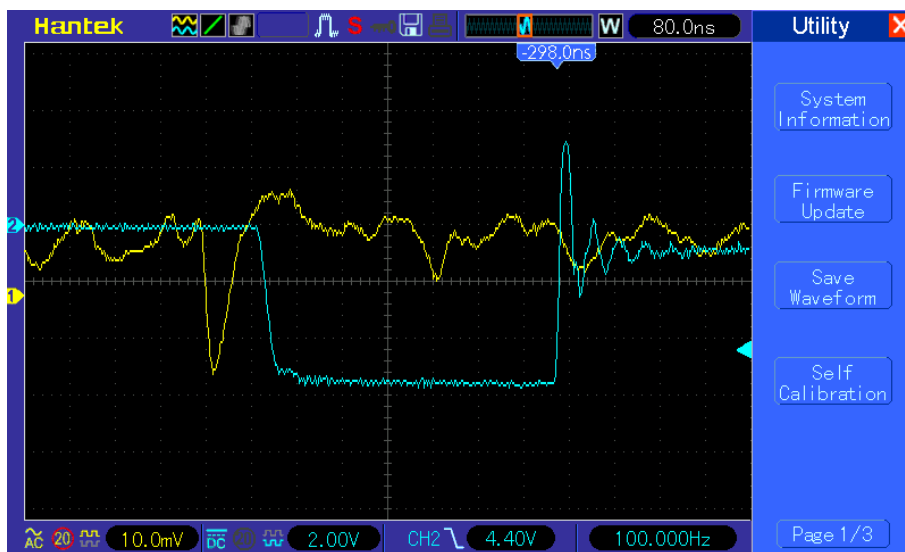


Figure 5. The output waveform from the module, measured with an oscilloscope. The digital pulse (blue) was converted from analogue (yellow) to TTL (inverted) standard for counting and triggering purposes.

The spectrum recorded with the ^{137}Cs gamma source is presented in Figure 6. The energy resolution for the 662 keV ^{137}Cs gamma yield was quantified at $10 \pm 0.3\%$ for the detector based on MAPD and LYSO scintillator [24]. This level of precision aligns with the registration of the 32 keV gamma signature originating from ^{137}Cs by the module. These observations collectively imply a notable reduction in electronic noise within the module. Beyond its economic viability, the module offers a combination of cost-effectiveness, compactness, and portability. Despite its economical construction, when scrutinized through a scientific lens, the module yields results of commendable quality that duly fulfill requisites.

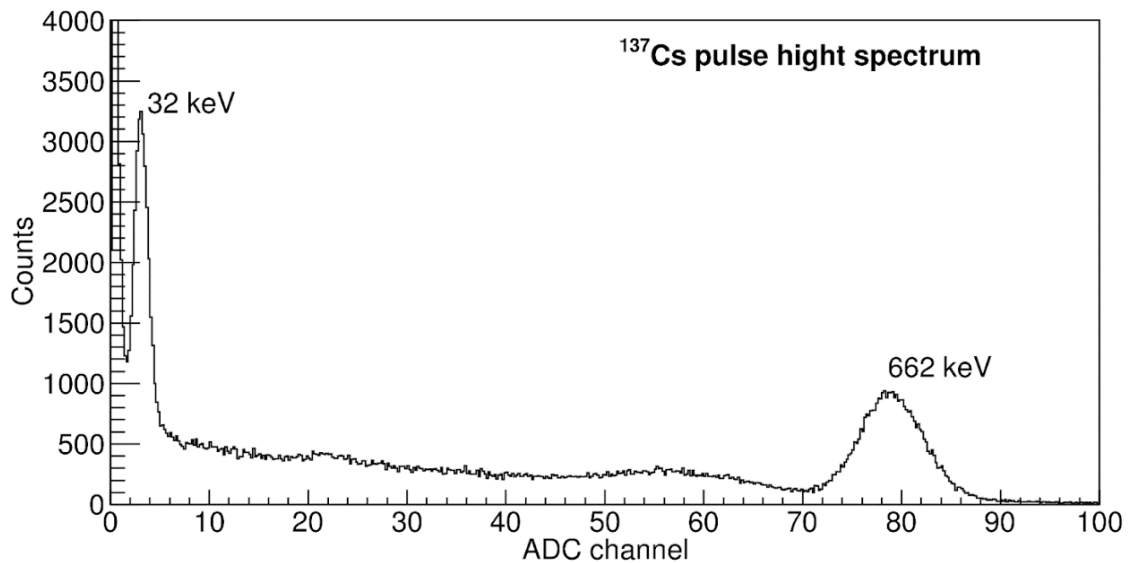


Figure 6. ^{137}Cs spectra on count and energy mode.

Conclusion

We have developed a cost-effective and efficient electronic module that integrates multiple electronic components, including a DC-DC step-up voltage converter, a preamplifier, and a comparator, into a compact circuit. It provides a bias voltage in the range of 30 V to 140 V with accuracy of 10 mV. The preamplifier linearly amplifies signals received from most scintillators commonly used in industry, medicine, and experiments, with decay times ranging from 30 to 100 ns. This module provides a sustainable and economical solution for detectors based on silicon photomultipliers and scintillators for ionization radiation detection, particularly for energy determinations and counting purposes. The module has been tested with a detector based on MAPD and LYSO scintillator using a ^{137}Cs gamma source. The energy resolution achieved was $10 \pm 0.3\%$ for 662 keV gamma rays. Counting performance of the module is approximately $2 \cdot 10^6$, considering a TTL output signal width of 450 ns. It is possible to reduce the signal width with minor modifications. The portability and compact design of this developed module make it a cost-effective and efficient solution that combines multiple functions.

Acknowledgments

This project has received funding from the European Union's Horizon 2021 Research and Innovation Programme under the Marie Skłodowska-Curie grant agreement 101086178.

References

- [1] Z. Sadygov et al., Phys. Part. Nucl. Lett. **17**, (2020) 160-176. [[CrossRef](#)].
- [2] Z. Sadygov et al., Phys. Part. Nucl. Lett. **10**, (2014) 780-782. [[CrossRef](#)].
- [3] S. Nuruyev et al., Nucl. Instrum. Methods Phys. Res. A: Accel. Spectrom. Detect. Assoc. Equip. **912** (2018) 320-322. [[CrossRef](#)].
- [4] F. Ahmadov et al., JINST **17** (2022) C01001. [[CrossRef](#)]
- [5] A. Sadigov et al., JINST **17** (2022) P07021. [[CrossRef](#)]
- [6] S. Nuruyev et al., JINST **15** (2020) C03003. [[CrossRef](#)]
- [7] A. Sadigov et al., Nucl. Instrum. Methods Phys. Res. A: Accel. Spectrom. Detect. Assoc. Equip. **824** (2016) 135-136. [[CrossRef](#)]
- [8] A. Sadigov et al., Nucl. Instrum. Methods Phys. Res. A: Accel. Spectrom. Detect. Assoc. Equip. **824** (2016) 137-138. [[CrossRef](#)]
- [9] F. Ahmadov et al., Funct. Mater. **24** (2017) 341-344. [[CrossRef](#)]
- [10] F. Ahmadov et al., Phys. Part. Nucl. Lett. **10** (2013) 778-779. [[CrossRef](#)]
- [11] G. Ahmadov et al., JINST **16** (2021) P07020. [[CrossRef](#)]
- [12] R.A. Akbarov et al., JINST **15** (2020) C01001. [[CrossRef](#)]
- [13] Dennis R Schaart, Phys. Med. Biol. **66** (2021) 09TR01. [[CrossRef](#)]
- [14] M. Ablikim et al., Phys. Rev. D **103** (2021) 112007. [[CrossRef](#)]
- [15] R. Akbarov et al., Nucl. Instrum. Methods Phys. Res. A: Accel. Spectrom. Detect. Assoc. Equip. **936** (2019) 549-551. [[CrossRef](#)]
- [16] F. Simon, Nucl. Instrum. Methods Phys. Res. A: Accel. Spectrom. Detect. Assoc. Equip. **926** (2019) 85-100. [[CrossRef](#)]
- [17] M. Casolino et al., Nucl. Instrum. Methods Phys. Res. A: Accel. Spectrom. Detect. Assoc. Equip. **986** (2021) 164649. [[CrossRef](#)]
- [18] Zh. Xie et al., Nucl. Instrum. Methods Phys. Res. A: Accel. Spectrom. Detect. Assoc. Equip. **1009** (2021) 165459. [[CrossRef](#)]
- [19] A.A. Nabiyeve et al., Nanomaterials **11** (2021) 2673. [[CrossRef](#)]
- [20] A.A. Nabiyeve et al., Polymer Degradation and Stability **171** (2020) 109042. [[CrossRef](#)]
- [21] S. Surti, Joel S. Karp, Phys. Med. **32** (2016) 12-22. [[CrossRef](#)]
- [22] F. Ahmadov et al., JINST **12** (2017) C01003. [[CrossRef](#)]
- [23] M. Holik et al., Scientific Reports **12** (2022) 15855. [[CrossRef](#)]
- [24] M. Holik et al., JINST **18** (2023) C01015. [[CrossRef](#)]